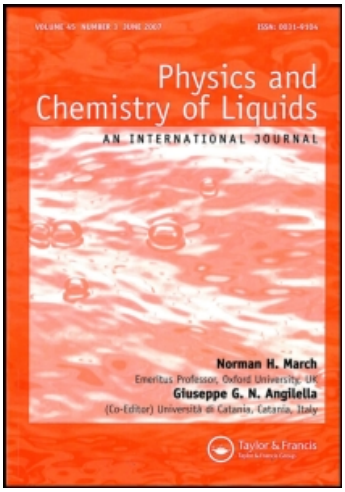

Physics and Chemistry of Liquids
Publication details, including instructions for authors and subscription information:
http://www.informaworld.com/smpp/title~content=t713646857

Lattice Models of Growth of Aligned Dipolar Fluids

O. Maas[ab]; D. M. Heyes[a]
[a] Department of Chemistry, University of Surrey, Guildford, U.K. [b] Department of Chemistry, Universität des Saarlandes, Saarbrücken, Germany

To cite this Article Maas, O. and Heyes, D. M.(1996) 'Lattice Models of Growth of Aligned Dipolar Fluids', Physics and Chemistry of Liquids, 31: 2, 109 — 125
To link to this Article: DOI: 10.1080/00319109608029564
URL: http://dx.doi.org/10.1080/00319109608029564

Phys. Chem. Liq., 1996, Vol. 31, pp. 109–125
Reprints available directly from the publisher
Photocopying permitted by license only

LATTICE MODELS OF GROWTH OF ALIGNED DIPOLAR FLUIDS

O. MAAS* and D. M. HEYES

Department of Chemistry, University of Surrey, Guildford, GU2 5XH, U.K.

(Received 1 July 1995)

The aggregation kinetics of a lattice model of aligned dipoles is examined as a simple model for electrorheological or magnetorheological fluids. We have found that the mechanism of cluster growth depends on time. Initial growth of clusters is dominated by monomer field-induced migration, but subsequent growth of the clusters at later stages is strongly dependent on monomer depletion and anisotropic diffusion of the aligned clusters.

We find that the mean size of the chain $\langle s(t) \rangle$ growth with time, t, according to $\langle s(t) \rangle \sim t^z$ with the exponent decreasing with increasing volume fraction, in accordance with recent experiments. This generic growth law is rather insensitive to the growth procedure of the model.

KEY WORDS: Electrorheological fluids, lattice model, simulation.

1 INTRODUCTION

Electrorheological, ER, and magnetorheological, MR, fluids can be used in various technological applications such as damping devices (for example, shock absorbers in automobiles) or clutch devices which transmit a torque. These fluids are colloidal dispersions of electrically (or magnetically) polarizable particles, with diameter ranging between 0.1 and 100 μm, in an insulating oil of low dielectric constant for the ER case. After the application of an electric/magnetic field on these fluids, there is often observed a dramatic increase in viscosity and the occurrence of a yield stress. This change in the rheological properties can take place in milliseconds and is reversible on removal of the field. This is known as the electrorheological or magnetorheological effect, which in both cases arises from a clustering of the colloidal particles to macroscopic dimensions. There are many technologically desirable characteristics for ER-fluids. These include low power consumption, rapid on/off characteristics, a wide working temperatue range ($-40 \rightarrow +200$°C). Moreover, ER-fluids should be stable, nonsettling, noncorrosive and nontoxic. In the case of the ER effect, an electric field polarises the particles. Three alternative mechanisms for this interfacial polarization have been proposed, (a) carrier migration through the bulk of the particle, (b) surface migration of carriers and/or (c) movement of the charges

*Permanent address: Department of Chemistry, Universität des Saarlandes, D66041 Saarbrücken, Germany.

held in a double layer with the counterion in the liquid phase[5]. This polarization leads to the formation of a field aligned dipole moment on the particles, which enables aggregation of the particles and an enhancement of the viscosity and development of a yield stress. The uncertainty in the precise interaction force between the colloidal particles in the ER fluid has made the MR fluids increasingly popular for model experimental studies in recent years.

A basic issue of importance for the development of effective commercial ER and MR fluids is the mechanism of growth of the clusters. Ideally they must aggregate as quickly as possible on application of a field and also break up again on removal of the field. "Responsiveness" and strength of the clusters are therefore important issues in optimising a commercial product. In the past simple models for dipolar have been used to represent ER fluids. We performed the first off-lattice (i.e., Brownian Dynamics) simulations of the ER effect[1-4]. In fact, model fluids interacting with dipoles superimposed on a repulsive core have proved to be useful models for the ER and MR fluids. These model fluids have received much analytic and simulation attention recently especially in the wider context of their phase diagrams, e.g.,[7-11]. One area which has attracted little attention concerns the initial stages of growth of the clusters from a random equilibrium starting state. It is this aspect of dipolar fluids that we consider here. The objective of this study is to gain some insights into the mechanism by which dipole colloidal fluids (whether ER or MR) grow to macroscopic dimensions. This ultimately could have implications for the "design" of more 'responsive' commercial fluids.

2 SIMULATION DETAILS

The model discussed here assumes that there are only dipolar interactions between the dispersed particles. The interaction energy between two spheres separated by $\underline{r}$ with an angle θ between $\underline{r}$ and the field direction, assumed to be y here, is, $V(r, \theta)$ where,

$$V(r, \theta) = -\mu_y^2(1 - 3\cos^2(\theta))/4\pi\varepsilon_0\varepsilon_r r^3 \tag{1}$$

where ε_0 is the permittivity of the vacuum, ε_r the relative permittivity of the fluid medium and μ_y is the field induced dipole moment, which is assumed to be proportional to the magnitude of the field, E. This interaction energy is anisotropic and leads to the aggregation of the polarized particles in fibrillar structures along the field direction (i.e., along $\theta = 0$). The fibrils eventually reach from one electrode to the other and thereby inhibit fluid flow, which causes an increase in the viscosity of the liquid. These structures have been observed many times for ER and MR systems, e.g.,[12,13,14,6]. There are advantages in using a lattice model here, as it gives us more control over the details of the dynamics of the particles. We can define arbitrary growth 'rules' and thereby establish the dominating processes taking place at various stages in the growth of real ER or MR clusters. We consider a square $N \times N$ 2D lattice, with fractional occupancy of particles, v being equivalent to the solids volume fraction in real liquids. Each occupied site represents one colloidal particle. A reduced

dimensionless temperature, T^*, is defined from the ratio of thermal and dipolar energies,

$$T^* = \frac{k_B T}{\mu_y^2/4\pi\varepsilon_0\varepsilon_r\sigma^3} \tag{2}$$

where σ is the diameter of a particle.

The interaction energy of the system is computed from the 8 nearest neighbour interactions on the lattice only, as indicated in Figure 1. Interactions from more remote sites are set to zero. Two particles cannot occupy the same site, as this represents severely overlapping particles, when the interaction energy for the two is $+\infty$. This infinite energy region of prohibited space is represented by the central black square in the figure. All energies are quoted in reduced units of $\mu_y^2/4\pi\varepsilon_0\varepsilon_r\sigma^3$. As can be seen the most favorable relative positions are for two 'lattice particles' to be situated along the y direction, with a weak attraction along the diagonal and a repulsion along the x direction. These values arise from applying Eqn. (1) to particles positioned at the centre of the lattice square. The distances are measured from the centre of the central square to the centre of the surrounding square. We denote this set of interactions to be of the type II lattice class. We also show in Figure 1

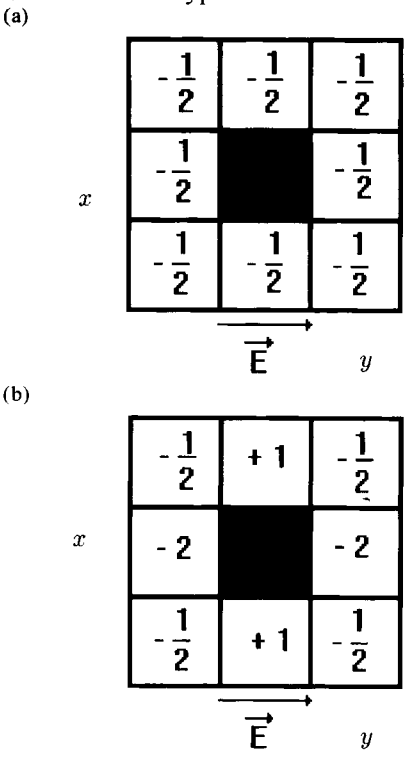

Figure 1 The nearest neighbour interactions used in the Monte Carlo simulations. The interaction energy with a central particle represented by a balck square is shown. Non-zero interactions are restricted to nearest neighbours. The energies are in units of $\mu_y^2/4\pi\varepsilon_0\varepsilon_r\sigma^3$. Key: (a) for model I shows a 2D lattice of isotropic interactions, and (b) shows model II interactions for a lattice of dipoles all pointing in the vertical (y) direction.

another set of lattice interactions (called type I) in which each surrounding site has the same interaction energy, $-1/2$, which is the average of that of the eight sites of dipole lattice II. The reason for the interest in this lattice, is we sought to establish and distinguish the effects of an anisotropic interaction from those of a symmetrical short range attractive interaction, having the same mean interaction energy in both cases.

We have used a standard Metropolis Monte Carlo scheme to evolve the system under the influence of an applied field[15]. The particles are first randomly placed on the lattice. In order to generate more realistic cooperative motion, we attempt to move *all* the particles at each stage in the simulation. As particles 'jump' a distance of order their diameter, σ, then phase space is traversed more efficiently than would be the case for a Brownian Dynamics continuum space model, in which jumps of $\sim 0.01\sigma$ are typical. This course-grained resolution is particularly well suited to follow the later stages of cluster growth.

We have adopted two different schemes for moving the particles. In method A we give all particles the chance to move at each step in the simulation, as illustrated in Figure 2. When the monomers attach to the ends of a chain they are also free to detach. This because all particles are treated independently from each other in the MC scheme. Therefore clusters once formed can subsequently break up. They are more likely to break up by loss of a monomer from the ends than from the loss of a monomer from the middle (i.e., by translating in the x-direction) as the former process has a lower energy penalty associated with it. Another consequence of this diffusion mechanism is that movement of large clusters as whole units is very unlikely. This is because such a process would involve the simultaneous displacement of all monomers in a cluster in the same direction at the same time, which is increasingly unlikely as the clusters grow in size. The dynamics scheme A therefore corresponds to the limit of a high viscosity host liquid, in which large cluster diffusion is essentially arrested on any useful timescale. The probability of a particle moving is given by the product of a spatial factor (diagonal movements are $2^{-1/2}$ less likely than along the x or y directions) and the usual Metropolis energy criterion.

In model B, which is also illustrated in Figure 2, the i-mers can move freely as whole units. Once formed the clusters are not allowed to break up. Instead they are treated as a single 'monomer' for the purpose of determining the particle trajectories. This is a valid approximation at low temperature, but an extreme limit of the real (i.e., experimental) behaviour at high temperature. For cluster diffusion we assume that the 'diffusion coefficients' (i.e., jump probabilities) in the x and y directions are inversely proportional to the area the cluster presents to the liquid in the y and x directions, respectively. The diffusion coefficient is equal to that of the monomers, D_0, in the y direction. This is because in this direction the clusters only present the area of a single monomer to the solvent. In contrast, in the x-direction diffusion is inversely proportional to the length of the cluster in the y direction, which leads to $D = D_0 i^{-1}$, where i is the number of monomers in the cluster along the y axis. (Clusters are deemed to be linear lines of monomers in the y direction, and any 'branches' in the x-direction are ignored.) This modification is meant to introduce some aspects of the diffusional behaviour of the real ER or MR fluids, in which resistance to cluster diffusion will be greatest perpendicular to the axis of the chain. In diffusional model B the clusters are not allowed to disintegrate, so aggregation is

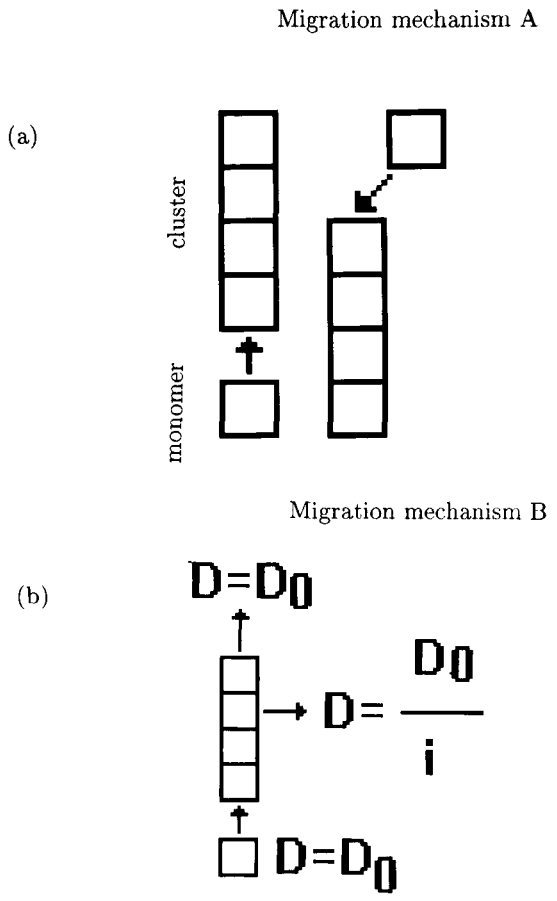

Figure 2 A diagram illustrating the two rules adopted for particle migration. No two particles can occupy the same site. In model A, shown in (a), the isolated particles or 'monomers' are allowed to diffuse irrespective of their status in or out of a cluster. In model B, shown in (b), vertical clusters formed out of i monomers can diffuse, anisotropically only as a single unit. Clusters, once formed cannot break up.

irreversible. This approximation is often applied in computer studies of aggregation, and has been used before for another lattice model of particles with an anisotropic potential[16]. It would also be realistic for the clusters to be in dynamic equilibrium with the pool of monomers and other clusters. However, the model would then have been prohibitively expensive to implement and also the results been obscured by the presence of several competing processes present in the same model. Rather our intention has been in this pilot study to explore systematically cluster growth and diffusion of limiting models for aligned dipole fluids. Models A and B are extremes of behaviour to which real ER or MR liquids will conform to under certain experimental conditions. Model A is most realistic at low fields (or equivalently high temperatures) and high volume fractions (where large cluster diffusion is perhaps not so important). Model B is most appropriate at high fields

or low temperature (i.e., in which there is low cluster break up probability) and low volume fraction. The two parameters we explored in our calculations were volume fraction and reduced temperature (which is proportional to E^{-2}, where E is the field).

3 RESULTS AND DISCUSSION

Instantaneous 2D pictures of the particle positions are informative and we therefore show some representative examples for models IIA and IIB computed on a 20×20 lattice in Figure 3. Periodic boundary conditions are applied to the systems, so that a particle leaving the cell enters through the opposite face[15]. The system is essentially infinite but with a periodicity length (scale) of 20 lattice units. At high temperature, e.g., $T^* = 10$ the IIA systems are highly disordered. This is because the attractive interactions are weak compared with thermal energy, and therefore there is a dynamic equilibrium between the clusters, involving accretion and decomposition. As temperature decreases, there is a greater driving force for monomers to attach to the ends of existing clusters and consequently the clusters grow in length. Nevertheless, even at the very low temperature of $T^* = 0.1$ there are still quite a few monomers and dimers in the system. There is a much wider distribution of cluster sizes than at the higher temperature. In the model IIA systems, the effective lack of diffusion for the large clusters greater than several monomers in length results in a structurally arrested state, which has similarities with a gel or glassy phase in experimental systems.

In contrast, the behaviour of the IIB systems is quite different. We see a greater degree of clustering, even at high temperatures. The clusters can diffuse and are thereby more effective at growing to longer lengths. (As discussed above, this is probably a little unrealistic, as large clusters in real ER or MR fluids would be in a dynamic state of growth and decay at $T^* = 10$.) However as the temperature decreases, the model becomes more realistic and we start to see many large clusters in the cell. They do not show any inclination to form 'thick' clusters as is observed in the later stages of aggregation in real ER or MR systems[13]. This effect is however likely to be influenced by quite subtle lateral (*i.e.*, x-direction) long range interactions and local restructuring which are not accounted for in this simple interaction model in which the local structure is highly idealised.

We also calculated properties averaged over many instantaneous 'snapshot' structures from the simulation. In Figure 4 we show the average energy per particle, $\langle e \rangle$, for the isotropic potential model I and using the A dynamics rule.

$$\langle e \rangle = \frac{\sum_{k=1}^{M} \sum_{i=1}^{N} e(k,i)}{MN} \tag{3}$$

where $e(k,i)$ is the interaction energy of the ith lattice site at the kth state, M is the number of MC moves and N is the number of particles in the box. The figure shows that the energy monotonically decreases from zero at zero volume fraction to -4 at

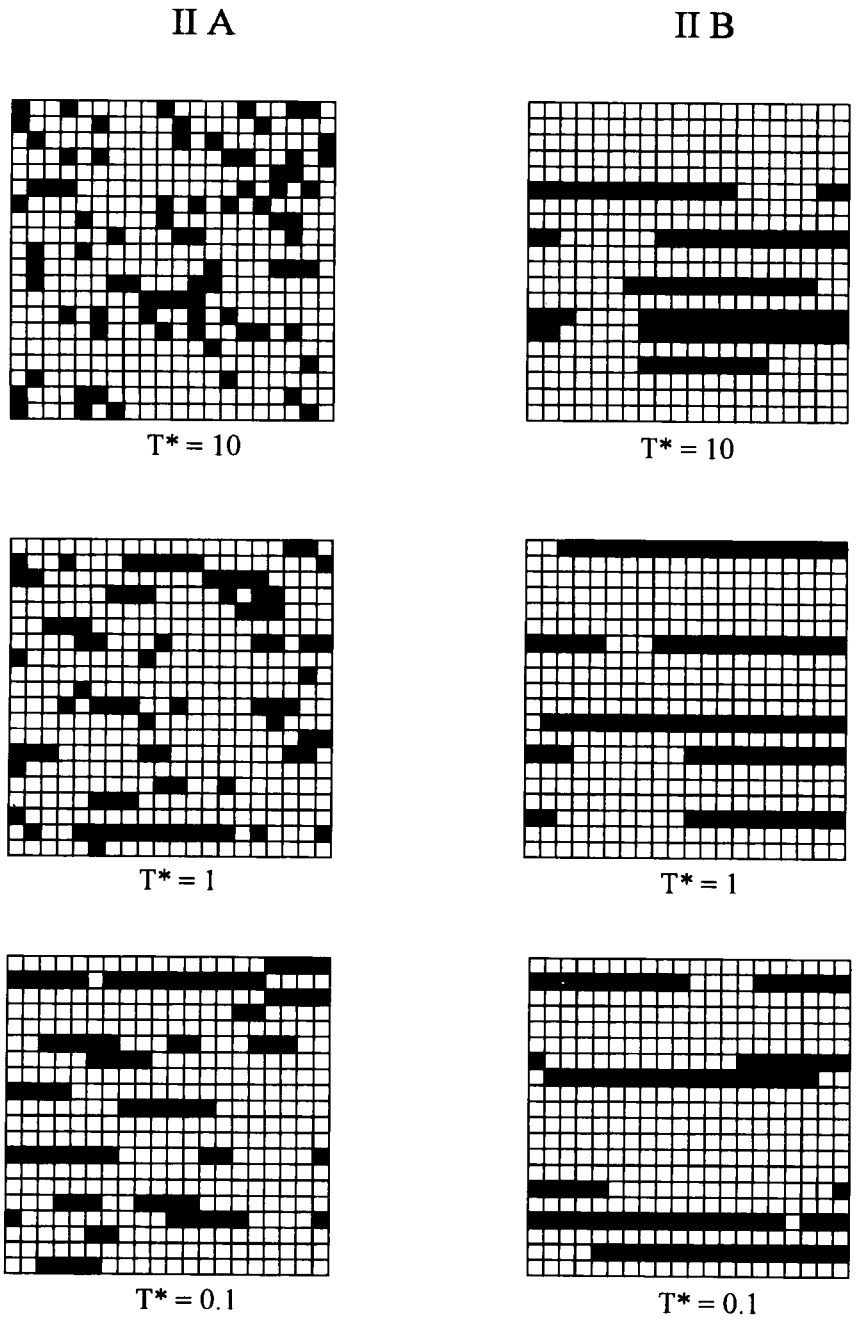

Figure 3 Snapshot configurations for 20 × 20 lattices of models IIA and IIB at a selection of reduced temperatures.

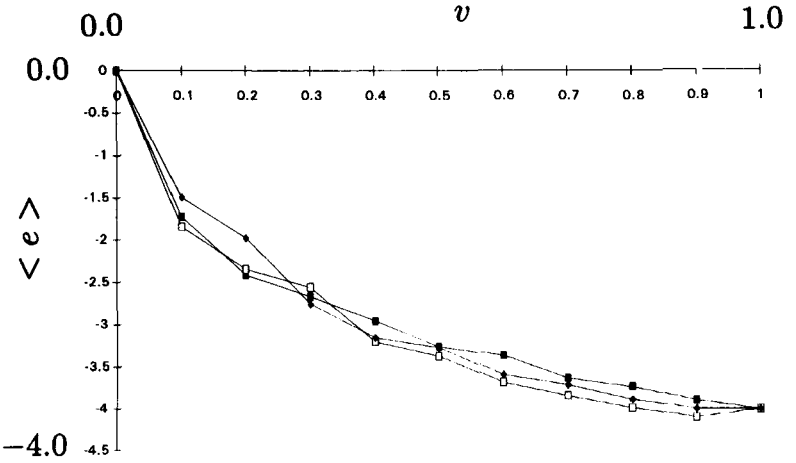

Figure 4 Average energy per particle $\langle e \rangle$ as a function of volume fraction and temperature for the symmetric model IA.

$v = 1.0$ for a fully occupied lattice, as expected based on random occupancy of the lattice sites. The curves are relatively insensitive to temperature over the wide range $0.1 < T^* < 10.0$, which we attribute to an underestimation of the level of cluster growth of this model at low temperature.

In contrast, for model IIA (Fig. 5) we observe a much greater sensitivity to temperature, especially at intermediate volume fractions. In particular, at lower temperature, the energy drops more steeply in the $0.1 - 0.2$ volume fraction range.

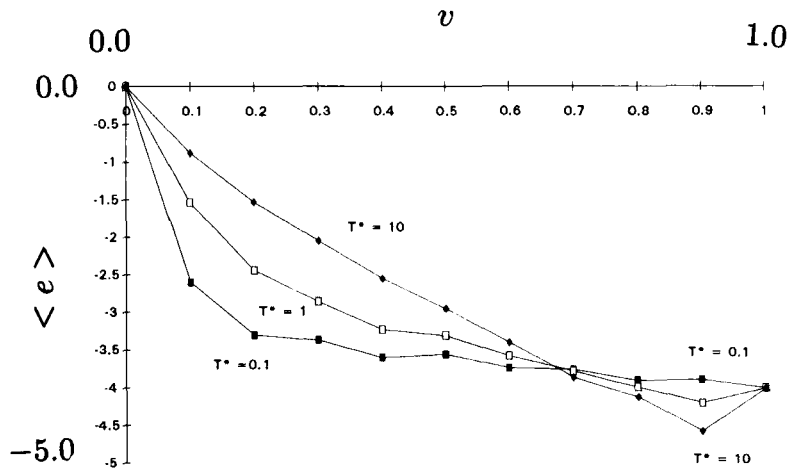

Figure 5 As for Figure 4, except model IIA is considered.

The lower temperature systems have a more negative interaction energy. This we attribute to the enhanced degree of clustering that occurs by virtue of attraction between the dipoles along the field direction and the ability of the system to form large clusters by merging. We note that most commercial ER and MR fluids operate in the 20–30% volume fraction range. Interestingly, there is a cross-over of all of these curves at a volume fraction $\sim 2/3$, which could have some underlying statistical significance. There is also a great temperature sensitivity at very high volume fraction $\sim 90\%$, but with the reverse order to that seen at lower volume fractions. At low temperature the energy per particle is rather flat above a volume fraction of 0.2. At higher temperature the energy per particle reaches a maximum of -4.5 at $v = 0.9$, which is geometrically possible if neighbouring sites in the x-direction are absent. It would be appear to be easier to achieve this state at higher temperature, which could indicate that a highly cooperative organisation of the system is required to form this state, which is only possible at high temperature.

In Figure 6 we show the corresponding IIB simulation phase diagram. This is quite different to that of both IA and IIA, which we attribute to the fact that the clusters are mobile and can coalesce to form linear chains. Each particle will have -4 energy units, and for long clusters end-effects contribute a negligible amount to the average. (Thin) chain formation is essentially complete at $v = 0.1$ for this system. The energy at volume fractions in excess of 0.1 is basically constant, although it becomes slightly more positive initially for $v > 0.1$. This is because at volume fractions in excess of $v = 0.1$ there are large clusters that are unable to percolate as they are separated from each other by existing percolating clusters, and therefore are isolated, unable to achieve the critical length required to percolate. This causes there to be a small shift to more positive energies above $v = 0.1$, because the end effects bring down the average energy per particle. This effect is an artefact of a two dimensional model, as in 3D the clusters would be able to grow by bypassing the existing percolating clusters.

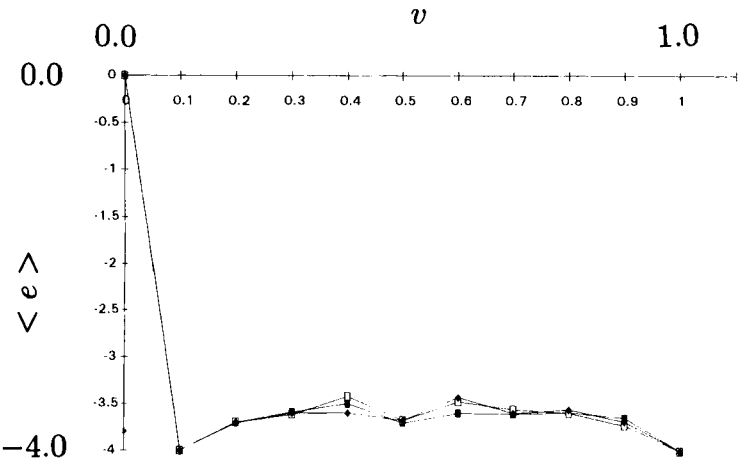

Figure 6 As for Figure 5, except model IIB systems are considered.

We have established that the mobility of the clusters, and the anisotropy of the potential field has a pronounced effect on the structures that form and their associated thermodynamic characteristics. Although these are non-equilibrium systems, because the dipoles are all aligned in the same direction, they can still achieve a steady state and it is justifiable to define an equation of state in this situation.

Cluster growth is conveniently described within the framework of percolation theory. The formation of 'infinitely' spanning or percolating chains across the system could be a defining feature of practical ER devices. If the clusters span the electrodes, the viscosity of the liquid will increase dramatically. We have computed the percolation characteristics of these model dipolar systems. A cluster is defined as one in which the monomers are joined together in a line along the y direction. (Side-branches in the x direction are not counted as being significant.) Percolating clusters are those clusters that cross the whole simulation cell in the y direction. In Figure 7(a) we show the fraction of generated configurations that percolate for a

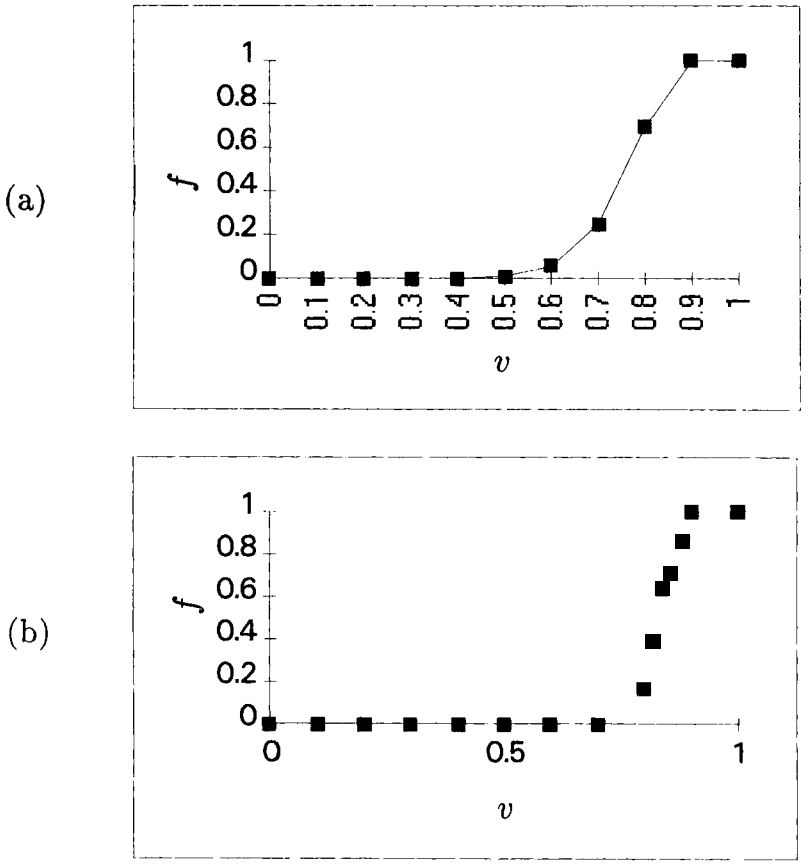

Figure 7 The fraction of MC generated configurations that have at least one percolating cluster as a function of volume fraction and at a temperature $T^* = 10$ for a IIA lattice. Key: (a) a 10 × 10 lattice and (b) a 20 × 20 lattice.

10×10 IIA lattice (i.e., anisotropic potential and all-monomer diffusion) at a reduced temperature of 10. Figure 7(b) presents the corresponding figure for a 20×20 lattice. The value of the percolation threshold is usually best estimated as the volume fraction at which 0.5 of the generated configurations have at least one percolating cluster. (In these 'directional' materials, there can be many percolating clusters.) The percolation threshold is relatively insensitive to the size of the cell, but the transition region in volume fraction over which the probability of percolating goes from zero to one becomes narrower as the size increases. This is consistent with the results of lattice and off-lattice equilibrium percolation studies[17,18]. The percolation threshold decreases as the temperature decreases (or equivalently the field increases). This is illustrated in Figure 8, in which we plot the percolation threshold for a 10×10 IIA lattice as a function of $1/T^*$. For intermediate inverse temperatures ($0.5 < T^{*-1} < 1.6$) the percolation threshold is approximately linear with T^{*-1} with a slope of -0.32. The percolation threshold is therefore proportional to E^2 over a limited field range. In contrast, the percolation thresholds for the IIB system are very different and much sharper than for the IIA systems. In contrast to the IIA case, in IIB the percolation threshold depends on the size of the simulation cell and is only weakly dependent on the temperature. This is because the clusters will eventually merge together to form the lowest energy state, as it is an irreversible process. For example, 10 particles on a 10×10 lattice will eventually form a percolating cluster. The percolation threshold is therefore a step function in volume fraction at $v = 0.1$. As the clusters, once formed, cannot break up, there is no temperature dependence for the percolation threshold for the IIB lattice.

The number of clusters of size s, $\langle N(s) \rangle$

$$N(s) = \frac{\sum_{t=1}^{N} N(s,t)}{M} \tag{4}$$

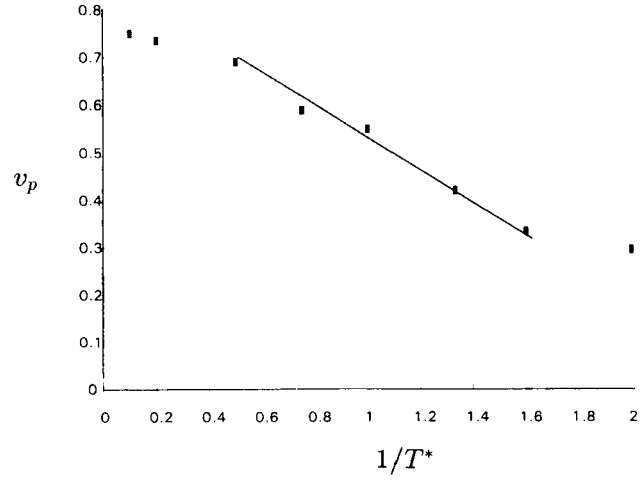

Figure 8 The temperature dependence of the percolation thresholds for a 10×10 IIA lattice.

was calculated after an equilibration period of 500 MC steps and was then averaged over a further sequence of 500 MC steps. In Figure 9 we show $\langle N(s) \rangle$ for a 10×10 lattice, at two state points. This function decays approximately as $s^{-\tau}$ where $\tau \sim 1.5$, which is somewhat lower than the universal value for equilibrium percolation (2.05 in 2D [17]).

Having established some steady state aspects of these systems, we now consider the mechanism of growth and associated kinetics. The mean cluster size was calculated using,

$$\langle s(t) \rangle = \sum_s s^2 N(s,t), \tag{5}$$

as used by Miyazima *et al.*[16]. This choice of a weighted average gives more importance to the larger clusters. In Figure 10 we show $\langle s(t) \rangle$ for a low temperature IIA state at the percolation threshold with $T^* = 0.25$ and $v = 0.25$. The time development of the mean cluster size shows three almost linear regions. There is a rapid increase in cluster size, followed by another region of smaller slope, and then a plateau of zero slope. As temperature increases the same regimes exist, however they are shifted to larger numbers of MC moves. The slopes are also lower at high temperature, indicating a more gradual growth. Examination of the particle dynamics reveals that the first region of rapid cluster growth is dominated by the diffusion and aggregation of isolated monomers to the ends of existing clusters. The second region of much slower growth is also caused by monomer migration, but as the monomers have further to diffuse on average by this time, the growth rate is slower. In the flat region, all the monomers have been exhausted and cluster growth essentially ceases. At higher temperature, there is more fluctuation of the data points (Fig. 10(b)) about the same overall trend, as particles are in a state of dynamic

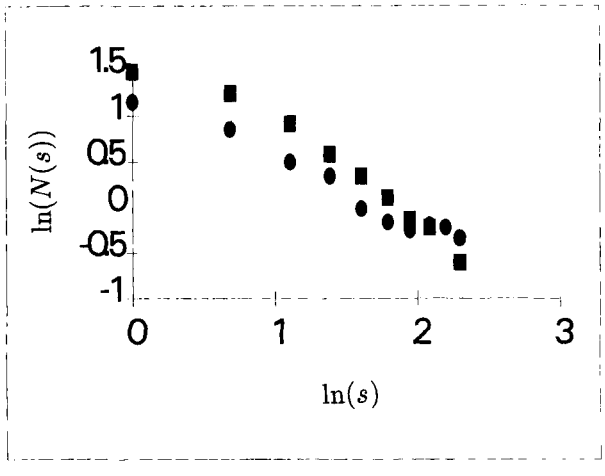

Figure 9 The cluster number distribution function for a 10×10 IIA lattice at two temperatures $T^* = 5$ (squares) and $T^* = 1$ (circles) at a volume fraction of 0.735 and 0.55, respectively.

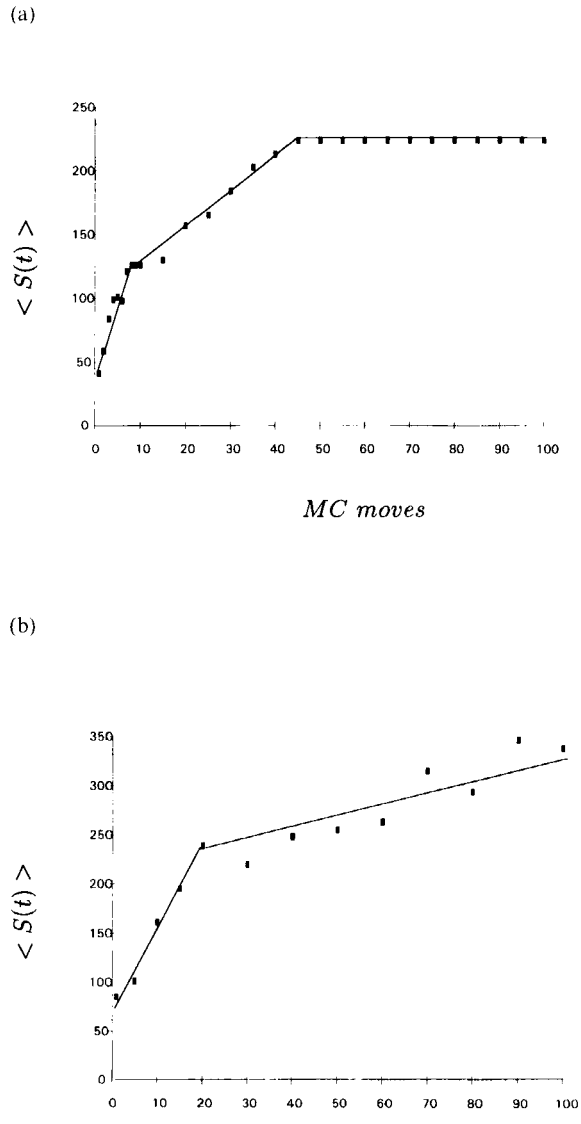

Figure 10 Mean cluster size as a function of number of MC moves for system states given on the figure. Key: 10 × 10 IIA lattice at (a) $T^* = 0.25$ and $v = 0.25$ and (b) $T^* = 0.55$ and $v = 0.295$. Both are at their percolation thresholds.

equilibrium in which particle detachment from the ends of the clusters is more frequent. Nevertheless, eventually $\langle s(t) \rangle$ shows some evidence of becoming statistically independent of time.

In Figure 11 we show $\langle s(t) \rangle$ for a low temperature IIB state at $T^* = 0.25$ and $v = 0.25$ (the same as Fig. 10(a)). This is not the percolation threshold for the B diffusion mechanism, as discussed above. Nevertheless, there are also three distinct regimes in time, as for the IIA case. The first region is basically the same process as for IIA, i.e., caused by the diffusion and clustering of monomers. The first region takes fewer MC moves to complete as the temperature decreases.

The second region is, however, quite different in origin, and is caused by the diffusion and merging of the small clusters. There are almost no monomers left in this second region of growth (see Fig. 12). The third 'region' reflects the slowing down of the growth of the clusters as the mean size increases and their diffusion rate diminishes. We note that the mean size is larger in the IIB case than for IIA at the same number of moves. This is because at a particular temperature in the IIA case there are still some small clusters when the growth process has essentially come to a halt, whereas in IIB cluster, cluster aggregation gives rise to additional growth.

The mechanism of cluster growth involves a random-walk and a merging of clusters when the two ends come together (side-to-side amalgomation is rare). This behaviour follows closely what is observed experimentally, recently demonstrated by performing visualisation experiments on paramagnetic colloidal particles[6]. Both models A and B show a decrease in growth rate with time, which can be conveniently represented by a growth law of the form, $\langle s(t) \rangle \sim t^z$ where $z < 1$, a relationship that is also observed experimentally. Figure 13 demonstrates that the simulation systems IIA also grow according to this power law. The value of z decreases with increasing volume fraction, in agreement with the experiments[6].

These experiments have also revealed some evidence that the growth of $\langle s(t) \rangle$ can be collapsed onto a single curve with a dimensionless time, t/t_B where a characteristic time $t_B \propto T^*/v$. Although this law was found to break down at high volume

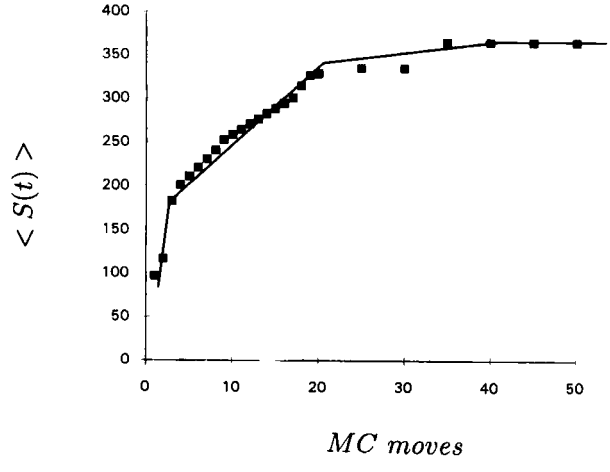

Figure 11 The same volume fraction and temperature as for Figure 10 (a) except that the IIB lattice was used.

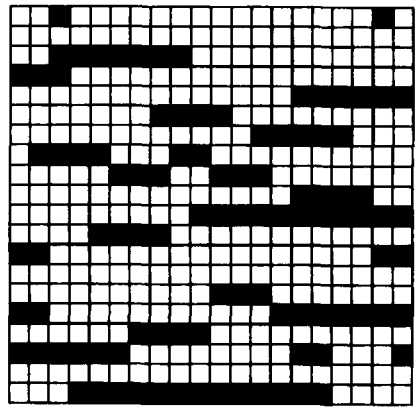

E →

Figure 12 Instantaneous configuration of the IIB lattice caught at the end of the first linear region in Figure 11.

fractions, suggesting a different growth mechanism. We did not have much success with this reduction, which could be because the experimental studies were carried out at much lower volume fractions (i.e., $\sim$ 0.001) than those considered here.

The main disadvantage with the Monte Carlo method is that a time scale is not clearly defined. The time corresponding to a MC move depends on the reduced temperature. At high temperature i.e., $T^* \gg 1$ the anisotropic interaction is of minimal importance and therefore the evolution of the system is diffusion dominated. If we assign a MC move with the diffusion of a particle through a particle diameter, σ i.e., $\sigma^2 = 2D\Delta t = 2k_BT\Delta t/3\pi\sigma\eta$ where Δt is a 'time step' associated with a MC move, η is the viscosity of the liquid in the absence of the field. Then we have that 1 MC move is equivalent to $3\pi\sigma^3\eta/2k_BT$. For particles of diameter $\sim$0.1 μm, the time step is equivalent to $\sim$ 1 s. The real time scale is strongly dependent on σ.

However, at low reduced temperatures, $T^* \ll 1$, the anisotropic interaction dominates the time scale and hence the value of Δt. The time for a particle to move through σ assuming Stokes law and classical electrostatics is $\sim 2\pi\eta/(E/MV\text{m}^{-1})^2$s which is independent of σ and typically $\sim$ ms for $E \sim MV\text{m}^{-1}$ [19]. For a typical mineral oil the time scale Δt here is $\sim$ 0.1 s. In practical applications the time to achieve maximum viscosity is typically seconds which is of the same order of magnitude as we observed in our simulations (i.e., 20–40 MC moves)[20]. Most ER devices operate in this very low reduced temperature regime where field induced migration of the colloidal particles dominates the motion and particle diffusion by Brownian motion is unimportant[19].

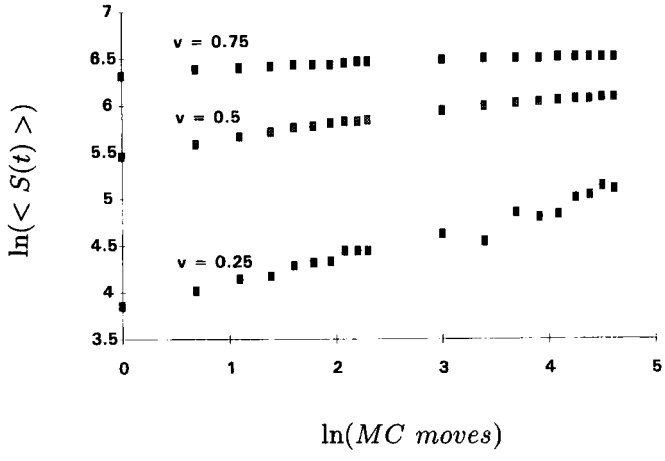

Figure 13 Plot of $\ln(\langle s(t)\rangle)$ vs. $\ln(t)$ for the IIA lattice on a 10×10 lattice at a temperature of $T^* = 0.25$. The volume fractions v are given on the figure.

4 CONCLUSIONS

In this report we have proposed a simple lattice model for ER and MR fluids. We have concentrated on the growth of the clusters when the field is suddenly turned on. We have explored the behaviour of two models, one of which emphasises monomer diffusion and has very slow diffusion for larger clusters. The other model favours irreversible cluster formation.

Taking account of the results of both models, we have shown that increasing the field decreases the volume fraction of particles that is needed to form a percolating cluster. In both models, initial cluster growth is determined by the rate of field promoted monomer migration and also the particle volume fraction. A subsequent slowing down of growth is caused by a depletion in the monomer concentration and an increase in the mean intercluster distance. The mean distance a monomer or cluster must travel in order to form a larger cluster increases. The rate of growth of the mean cluster size decreases with time and follows the same generic power law as observed in experiment. This analytic form was followed by both models, and consequently it is not very sensitive to the growth model chosen. The growth law $\langle s(t)\rangle \propto t^z$ is therefore not very useful in discriminating between different growth mechanisms.

Acknowledgement

O. M. thanks the European Commission's ERASMUS scheme for funding.

References

1. P. Bailey, D. G. Gillies, D. M. Heyes and L. H. Sutcliffe, *Mol. Sim.*, **4**, 137 (1989).
2. D. M. Heyes and J. R. Melrose, *Mol. Sim.*, **5**, 293 (1990).
3. J. R. Melrose and D. M. Heyes, *J. Chem. Phys.*, **98**, 5873 (1993).

4. J. R. Melrose and D. M. Heyes, *J. Coll. & Interface Sci.*, **157**, 227 (1993).
5. H. Block, J. P. Kelly, A. Qin and T. Watson, *Langmuir*, **6**, 6 (1990).
6. J. H. E. Promislow, A. P. Gast and M. Fermigier, *J. Chem. Phys.*, **102**, 5492 (1995).
7. M. J. Stevens and G. S. Grest, *Phys. Rev. Lett.*, **72**, 3686 (1994).
8. H. Zhang and M. Widom, *Phys. Rev., E*, **49**, R3591 (1994).
9. D. Levesque and J. J. Weis, *Phys. Rev., E*, **49**, 5131 (1994).
10. K. C. Hass, *Phys. Rev., E*, **47**, 3362 (1993).
11. M. J. P. Gingras and P. C. W. Holdsworth, *Phys. Rev. Lett.*, **74**, 202 (1995).
12. J. E. Martin, D. Adolf and T. C. Halsey, *J. Coll. & Interf. Sci.*, **167**, 437 (1994).
13. H. Conrad and A. F. Sprecher, *J. Stat. Phys.*, **64**, 1073 (1991).
14. C. Tsouris and T. C. Scott, *J. Coll. & Interf. Sci.*, **171**, 319 (1995).
15. M. P. Allen and D. J. Tildesley, *Computer Simulation of Liquids*, Oxford Univ. Press, 1987.
16. S. Miyazima, P. Meakin and F. Family, *Phys. Rev., A*, **36**, 1421 (1987).
17. D. Stauffer, *Introduction to Percolation Theory* Taylor & Francis 1985 London.
18. N. A. Seaton and E. D. Glandt, *J. Chem. Phys.*, **86**, 4668 (1987).
19. D. J. Klinenberg, F. van Swol and C. F. Zukoski, *J. Chem. Phys.*, **91**, 7888 (1989).
20. G. B. Thurston and E. B. Gaertner, *J. Rheol.*, **35**, 1327 (1991).